Control of Residual Thermal Stresses in Shape Deposition Manufacturing

R.K. Chin, J.L. Beuth, C.H. Amon
Department of Mechanical Engineering
and Engineering Design Research Center
Carnegie Mellon University
Pittsburgh, PA 15213-3890

Abstract

Layer-level thermal and mechanical modeling of the microcasting stage of Shape Deposition Manufacturing is presented. Thermo-mechanical models of carbon steel deposited onto a carbon steel substrate are described. Mechanics modeling addresses the issue of residual stress build-up. The effects of substrate heating and bending constraint on the build-up of residual stresses are shown. Results show that thermal cycling from newly applied droplets drastically changes the stress state in the top of the substrate. Originally unstressed regions go through an inelastic compression-tension stress cycle. Residual stresses reach values that may cause yielding in carbon steel. Moderate heating of the substrate above room temperature prior to droplet deposition reduces stresses significantly. Bending constraint during part manufacture allows partial relaxation of stresses as the constraint is removed.

Introduction

Shape Deposition Manufacturing (SDM) is a manufacturing process which allows the creation of complex three-dimensional parts by the successive deposition of layers of material. After each layer is deposited, it is machined to the required dimensions before depositing the next layer (Merz *et al.*, 1994). SDM combines solid freeform fabrication with other processing operations, such as multi-axis CNC machining, material deposition, and shot peening. The benefits of SDM include the ability to build parts with complicated geometries, multiple materials, and embedded components. Unlike conventional solid freeform fabrication processes, SDM can also directly build fully dense, functional metal parts to high dimensional accuracy.

Within SDM, a process for depositing layers is required. The principal deposition process currently in use is termed microcasting, in which droplets of molten material are deposited onto a much cooler substrate. Residual stresses arise when the hot droplet cools off while it heats up the material underneath, causing differential thermal strains. Undesirable effects of residual stress include warping, loss of edge tolerance, and delamination. Residual stress can also reduce the apparent strength and service life of a part. Residual stress build-up is inherent in any manufacturing process based on successive molten material deposition. Ultimately, to control the undesirable effects of residual stresses through process changes and part design changes, it is necessary to understand how such stresses build up during manufacture.

The goal of this work is to model microcasting on a layer level. The temperature distribution in the molten droplet and the substrate, and the stresses that build up in the droplet and substrate due to differential thermal strains, are investigated after the droplet spreads out until the temperature distribution becomes uniform. A one-dimensional thermal model is first presented and verified. The corresponding mechanical model undergoing thermal loads is verified by using an assumption of pure elastic behavior. Then a model incorporating creep and temperature-dependent properties is used to predict thermal stresses in microcasted configurations. The solution strategy is similar to that presented by Thomas *et al.* (1987) and by Zabaras *et al.* (1991). Finally, the stress reductions achievable from uniform heating of the substrate and constraint of the substrate are shown.

Thermal Model

Residual stress modeling has both a thermal aspect and a mechanical aspect. The approach used here is to solve the thermal problem first and to use then the temperature solution as an input to the mechanical model. In the mechanical model, loading comes from differential thermal expansions and contractions. Mechanically-induced temperature changes are assumed to be negligible. The ABAQUS finite element package is used in this study because of its capability to model both the thermal and mechanical problems.

The thermal model is shown in Figure 1a. The geometric parameters are the thicknesses of the droplet and substrate. The three initial temperatures of the model are the initial temperatures of the substrate, droplet, and interface. The bottom of the substrate is fixed at the initial substrate temperature. At the top of the substrate, boundary conditions corresponding to heat convection to the ambient and radiation from the plasma arc are imposed. The temperature-dependent conductivity, specific heat, and diffusivity used in the model (from Allard, 1969, and Touloukian, 1967) are those of a low-carbon steel.

To verify the accuracy of the thermal modeling, a typical finite element result is compared to an independent finite difference result from Amon *et al.* (1995). The specific parameters used by Amon *et al.* (1995) are shown directly in Figure 1a, except for the geometry and freezing parameters. The geometry is of a 1 mm layer deposited onto a 7 mm substrate, and the latent heat of fusion is 270,000 J/kg. In the finite difference model, the material solidifies at exactly 1773 K, while in the finite element model, the material has liquidus and solidus temperatures of 1775 K and 1771 K, chosen to correspond to a mean solidification temperature of 1773 K. Distinct liquidus and solidus temperatures are used to incorporate latent heat effects into an effective specific heat, and the 4 K difference between the liquidus and solidus temperatures is negligible. The comparison of the finite difference and finite element solutions for the temperature history at a point located 0.5 mm into the droplet (halfway between the top of the substrate and the top of the droplet) yields a maximum discrepancy of 30 K, which corresponds to 1.32% of the working temperature range of 303 K to 2573 K.

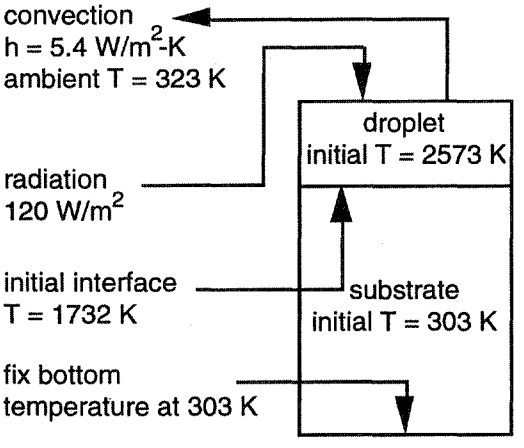

Figure 1a. Thermal Model.

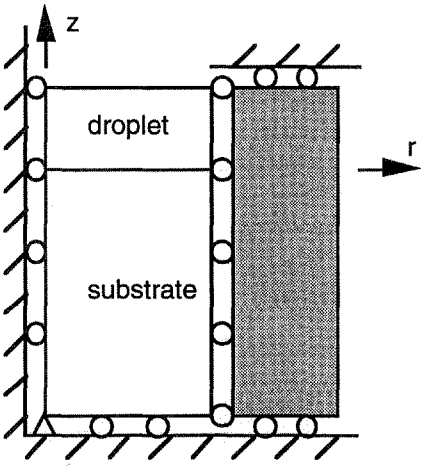

Figure 1b. Mechanical Model.

To match the geometry of a layer and substrate used during part manufacture, a thermal model of a 3 mm layer deposited on top of a 19 mm substrate is constructed. It consists of a uniform mesh of 220 one-dimensional first-order elements. The liquidus and solidus temperatures in this model are 1785 K and 1748 K, which are the estimated liquidus and solidus for a low-

carbon steel used in a part made by SDM. The other parameters are identical to those used to verify the thermal modeling. A mesh refinement study using three levels of resolution showed negligible changes in the temperature distribution when the number of elements was doubled or halved.

Figure 2 shows the temperature distribution through the layer and substrate at discrete times. The deposited layer corresponds to the positive axial coordinate while the substrate corresponds to the negative axial coordinate (see Figure 1a). The deposited layer cools down as time elapses while the substrate first heats up and then cools down. Heating is significant near the top of the substrate. The temperature near the top of the substrate increases hundreds of degrees K before beginning to cool. Substrate remelting, needed for good bond strength between the substrate and the deposited layer, is not predicted to occur for the combination of initial temperatures used. This one-dimensional model of layer deposition allows heat to flow in only one direction. It predicts a solidification time of 1.56 seconds. Steady-state is reached in approximately 70 seconds.

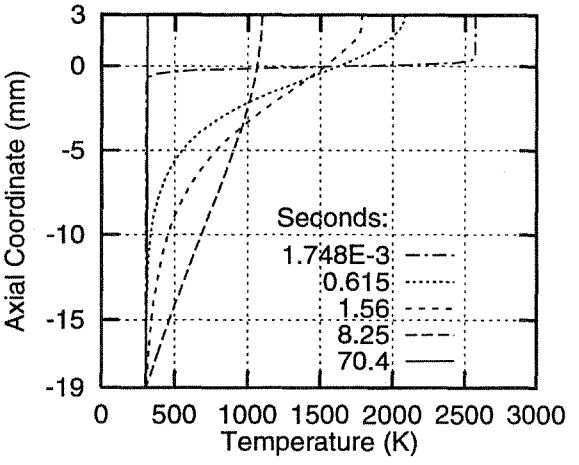

Figure 2. *Temperature distribution at selected times. Initial substrate temperature 303 K.*

Mechanical Model

To study the build-up of residual stresses, a mechanical model is formulated. The mechanical model has the same geometry as the thermal model (i.e., a 3 mm layer and a 19 mm substrate). Second-order axisymmetric elements are used in the mechanical model with appropriate boundary conditions applied to render the stress distribution a function of the axial coordinate only. As with the thermal model, a uniform mesh of 220 elements is used, and three levels of mesh refinement were tested to confirm sufficient mesh resolution.

The finite domain used for all the mechanical results presented in this work is shown in Figure 1b. A condition of zero axial (z) displacement is applied at the bottom of the model. This corresponds to a flat substrate and also prevents rigid-body motion in the axial direction. The body remains free to expand or contract in the axial direction. The centerline undergoes zero radial displacement while the outer wall is constrained to expand (or contract) uniformly in the radial direction. Because this model maintains straight vertical edges and a flat substrate bottom, it allows no bending deformation.

To model a deposited layer of indefinite extent, periodic boundary conditions are needed. Periodic boundary conditions require straight edges (but not necessarily vertical edges) on the finite domain to allow any number of the finite domains to fit together as they deform. While axisymmetric elements are used for the mechanical model, the periodic boundary conditions and

the absence of radial temperature variation ($\partial T/\partial r = 0$) lead to a biaxial stress state that can be described with only one stress component (either σ_{rr} or $\sigma_{\theta\theta}$) that is a function of the z coordinate only.

A mechanical solution which assumes linear elastic behavior with temperature-independent mechanical properties (Young's modulus, Poisson's ratio, and thermal expansion coefficient) in the droplet and substrate is used to verify the correct use of ABAQUS to solve the mechanical portion of the problem. The purely elastic material model has a steady-state stress solution that can be expressed in closed form. Also, results from an elastic solution are easy to interpret, so this solution aids the interpretation of subsequent results including nonlinear deformation.

Figure 3 shows the stress (σ_{rr} or $\sigma_{\theta\theta}$ normalized) as a function of depth in the deposited layer and substrate at discrete times. There is no stress initially, but as the hot droplet cools, tensile stresses build up in the droplet. Meanwhile, compressive stresses build up in the substrate. There are two causes for compression in the substrate. First, the top of the substrate is restrained from expanding freely as it heats up. Second, the mechanical boundary conditions demand zero net radial force; this condition requires compression in the substrate to balance the tension in the newly deposited layer. A compressive stress remains even after the entire domain cools to room temperature. Because the deposited layer and the substrate undergo equal uniform strains and experience no external forces, the final stresses must be

$$\frac{\sigma_d\,(1-\nu)}{E\,\alpha\,\Delta T} = \frac{1}{1+\frac{d}{s}} \quad \text{and} \quad \frac{\sigma_s\,(1-\nu)}{E\,\alpha\,\Delta T} = \frac{-1}{1+\frac{s}{d}} \tag{1}$$

where σ_d = final radial stress in the droplet
σ_s = final radial stress in the substrate
E = Young's modulus
ν = Poisson's ratio
α = linear thermal expansion coefficient
ΔT = initial temperature difference between droplet and substrate
d = thickness of the droplet = 0.003 m
s = thickness of the substrate = 0.019 m

The final normalized residual stress values are predicted to be 0.86 in the droplet and –0.14 in the substrate, which agrees with the finite element result.

To predict stresses in microcasted parts, a model is formulated that incorporates a creep law, temperature-dependent Young's modulus, and temperature-dependent linear thermal expansion coefficient. To account for the effect of creep, a secondary (steady-state) creep law for a medium carbon steel in the austenitic phase is chosen (from Thomas *et al.*, 1987).

$$\dot{\varepsilon} = A\,(\sinh(B\bar{\sigma}))^n \exp\left(-\frac{C}{T}\right) \tag{2}$$

where $\dot{\varepsilon}$ = creep strain rate in reciprocal seconds
$\bar{\sigma}$ = Mises equivalent stress in MPa
T = temperature in K
$A = 907 \times 10^{10}$
$B = 0.0356$
$C = 41938$
$n = 6.9$

This creep law is a commonly used form based on activation energy arguments and is used by Thomas *et al.* (1987) to study casting problems. In the creep law (equation [2]), the interaction between the exponential factor and the hyperbolic sine effectively builds in a temperature-dependent yield stress with perfect plasticity (no hardening). At a temperature of 303 K, a stress

larger than 460 MPa will cause a high creep strain rate; the effective yield stress at 303 K is 460 MPa.

The piecewise-linear temperature-dependent Young's modulus used in the model is from data of Thomas *et al.* (1987) and approaches a value of about 25% of the room temperature value at the solidus temperature. At 303 K, the Young's modulus is 207.75 GPa. The temperature-dependent linear thermal expansion coefficient, ranging from 11.9 x 10^{-6}/K to 14.9 x 10^{-6}/K, is taken from the *ASM Metals Reference Book* (1981), where it is defined as the mean expansion between 293 K and T, where T ranges from 373 K to 973 K. Beyond that range, a constant value is used. The Poisson's ratio used in the model is a constant 0.27.

Figure 4 shows the radial stress distribution obtained at discrete times with temperature-dependent creep, Young's modulus, and thermal expansion. The tension in the deposited layer builds up slower than in the pure elastic case because creep at high temperatures does not permit high stresses. Very early, there is compression in the top of the substrate due to heating just as for the elastic case, although the magnitude is smaller than for the elastic case. As seen in Figure 2, heat conducted from the molten droplet into this region raises the temperature hundreds of degrees K. Inelastic straining occurs while the material is under compression at these elevated temperatures. After the material reaches its maximum temperature (which is different for each point), it begins to cool but is restrained from freely contracting. As this happens, the stress state turns to tension. The final stress distribution (see the solid line in Figure 4) consists of nearly uniform tension in the newly deposited layer, tension at the top of the substrate, and nearly uniform compression at the bottom half of the substrate. The compressive stress at the bottom of the substrate is a reaction to the tensile stresses in other portions of the droplet and substrate. The tensile region at the top part of the substrate indicates the depth of stresses due directly to thermal effects. The size of this affected region is 2 to 3 times the depth of the deposited layer.

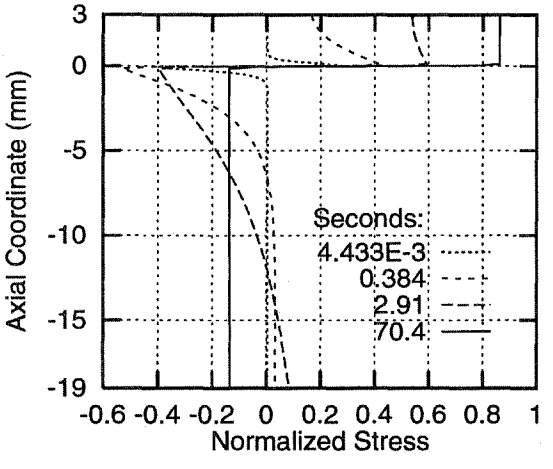

Figure 3. *Stress distribution - elastic behavior assumed; temperature-independent material properties.*

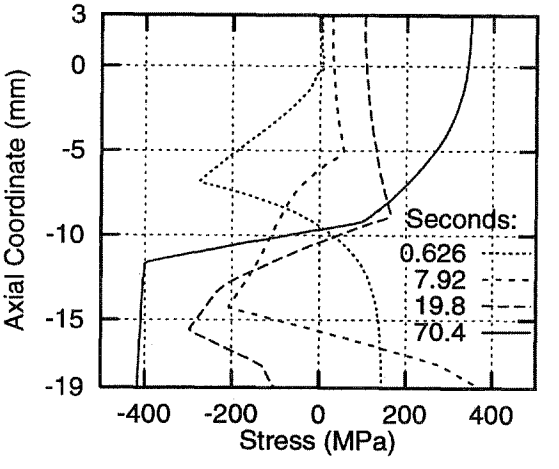

Figure 4. *Stress distribution - temperature-dependent inelastic material behavior.*

Substrate Preheating

One option for reducing residual thermal stress is to uniformly preheat the substrate. The cases considered thus far use an initial substrate temperature of 303 K. If a higher substrate temperature is used, then a reduction of residual stress can be expected. Preheating is common in welding applications. A quantitative answer is sought to the question of whether a moderate increase in substrate temperature can significantly reduce residual stresses in microcasting. Even

though substrate heating makes the manufacturing process more complex, a large benefit may justify the added complexity. Moderate uniform preheating may be practical, and examining uniform preheating also represents the first step toward examining local preheating in the future.

Two higher substrate initial temperatures of 473 K (200 °C) and 673 K (400 °C) are used to examine the potential benefits of heating the substrate. 473 K represents a moderate preheating of the substrate while 673 K represents a practical limit. At high preheating temperatures, problems may be encountered involving oxidation of the part exterior or coarsening of the highly desirable fine-scale microstructure achieved by rapid cooling of deposited layers.

The stress distributions for initial substrate temperatures of 473 K and 673 K are similar to the stress distribution for an initial 303 K substrate, except that the stress magnitudes are smaller. The steady-state final stress distributions corresponding to the three substrate temperatures investigated are shown in Figure 5. The 303 K stress distribution in Figure 5 is the same as the steady-state stress distribution from Figure 4. Heating the substrate to 473 K and 673 K reduces the magnitudes of the final stresses by about 150 MPa and 250 MPa, respectively, in the deposited layer and by about 200 MPa and 300 MPa, respectively, at the bottom of the substrate. Because residual stress build-up occurs at later times (i.e., at lower temperatures), moderate heating can reduce residual stresses significantly. The levels of uniform heating explored may be practical to implement.

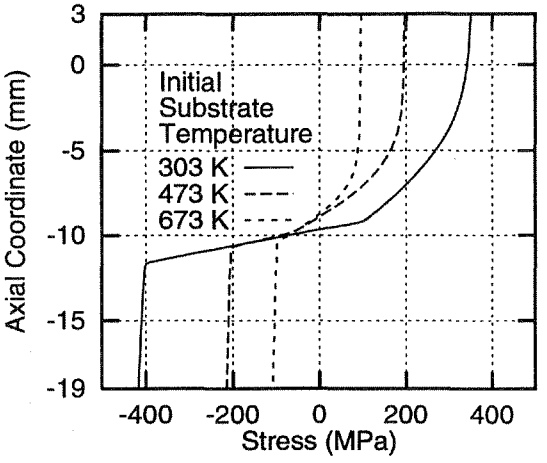

Figure 5. Final stress distribution for 3 different initial substrate temperatures.

Substrate Constraint

Although displacement constraints are usually associated with higher stresses, it is possible to use constraint in microcasting to actually lower the magnitude of the residual thermal stress. To determine the role of constraint, two loading configurations are examined. The mechanical boundary conditions sketched in the basic model of Figure 1b do not allow the substrate to bend, simulating bolts holding the substrate down against a pallet during part manufacture. Two new loading configurations are investigated and shown in Figures 6a and 6b. In Figure 6a, the model is constrained from bending during manufacturing (as in Figure 1b) but is then released. To simulate releasing (unbolting) the substrate after part manufacture, a moment of the same magnitude as the resultant moment that constrains the part from bending, but of opposite sign, is superimposed. It is added after the stresses during manufacture reach steady state. The superimposed moment is made up of a linear stress distribution that adds no net force and elastically deforms each point in the layer and substrate. In Figure 6b, the mechanical model is of a substrate that is permitted to bend during manufacture. The outer wall remains straight while it

displaces but is also allowed to rotate, resulting in no net applied moment. These boundary conditions represent microcasting without constraining the substrate during part manufacture.

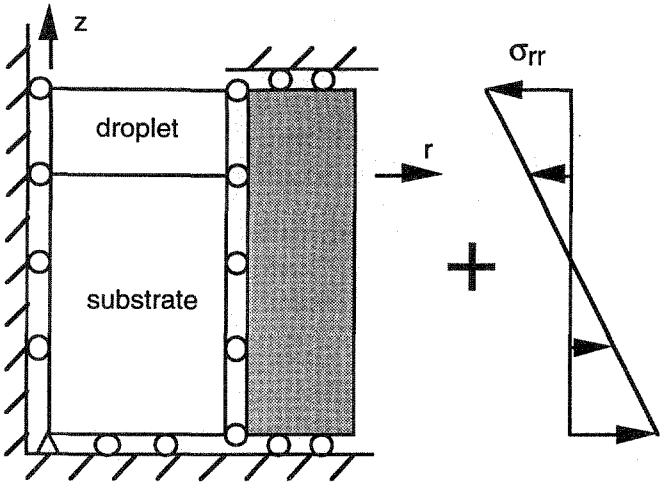

Figure 6a. Constrain from bending during manufacture, then release.

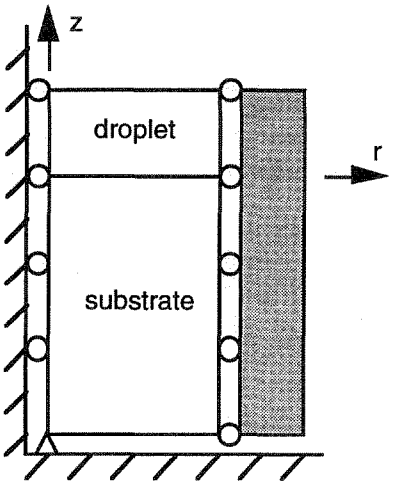

Figure 6b. Allow bending during part manufacture.

Figure 7a shows the stress distribution before unbolting, the superimposed stresses, and the stress distribution after unbolting for the problem of Figure 6a. The stress distribution before unbolting is the final stress distribution from Figure 4. The largest superimposed stresses are quite large (exceeding 500 MPa). In some locations, the sign of the stress changes after unbolting. For instance, unbolting changes the tension in the deposited layer to compression and the compression at the bottom 3 mm of the substrate to tension. Also, the peak stress magnitude decreases 200 MPa after unbolting.

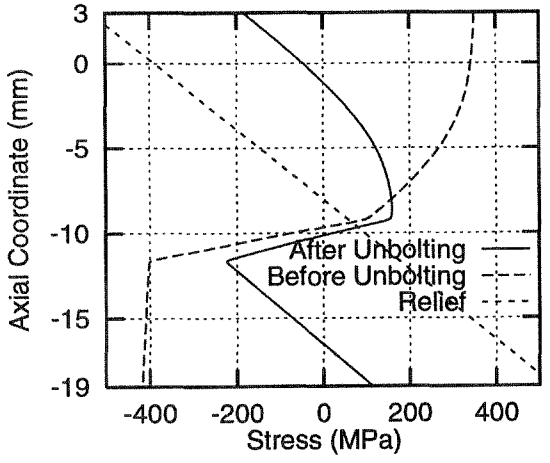

Figure 7a. Effect of unbolting on the residual stress distribution.

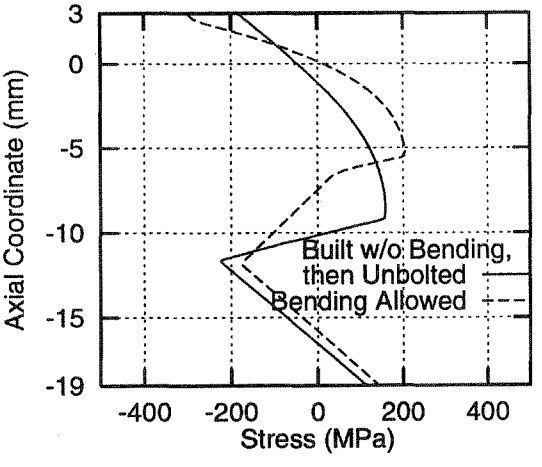

Figure 7b. Effect of allowing bending during part manufacture.

In Figure 7b, the final stress distribution in a substrate and layer built with constraint, and then unbolted, is compared to the final stress distribution in a substrate and layer built without bending constraint from bolting. At the top of the deposited layer, bolting reduces the stress magnitude by about 120 MPa. Bolting also reduces the stress magnitude at the bottom of the substrate. Furthermore, the difference between the largest tensile stress and the smallest compressive stress is 380 MPa when bending is not allowed versus a larger 505 MPa when

bending is allowed during manufacture. An additional benefit of bolting is the control of bending deformation. If the first layer is deposited without bending constraint, then the substrate and layer warp. When a second layer is deposited, curvature change is added to the warped configuration. Each additional layer causes the incomplete part to warp further. This problem will not appear if the part is restricted from bending during manufacture. Thus bending constraint from bolting to a stiff pallet is important for control of both residual stress and part warping.

Summary

This study has presented verified thermo-mechanical models for a single layer of carbon steel deposited onto an initially stress-free thick carbon steel substrate, simulating the effects of droplets of a microcasted part being deposited onto a thick substrate. The models show that the deposited layer causes significant substrate heating to a depth of 2 to 3 layer thicknesses. For a substrate that is initially at room temperature, thermal cycling and inelastic flow cause the deposited layer and the portion of the substrate that is significantly heated to reach very high stresses in tension. Preheating the substrate moderately (to 473 K) reduces the stresses significantly (by 200 MPa). Bending constraint during manufacturing is important for control of warping and because after manufacturing, the residual stresses are partially relaxed after the bending constraint is removed.

Acknowledgements

The authors gratefully acknowledge financial support by the Office of Naval Research under Grant No. N00014-94-1-0183. This work is also supported by the Engineering Design Research Center, an Engineering Research Center of the National Science Foundation, under Grant No. EEC-8943164.

References

Allard, S., (ed.), 1969, "Metals Thermal and Mechanical Data," "Metaux donnees thermiques et mecaniques," *Tables internationales de constantes selectionnees*, 16, Oxford, New York, Pergamon Press.

Amon, C.H., Schmaltz, K.S., Merz, R., and Prinz, F.B., 1995, "Numerical and Experimental Investigation of Interface Bonding Via Substrate Remelting of an Impinging Molten Metal Droplet," accepted: *Journal of Heat Transfer.*

ASM Metals Reference Book: A handbook of data about metals and metalworking, 1981, compiled by The Editorial Staff, Reference Publications, American Society for Metals, pp. 167.

Merz, R., Prinz, F.B., Ramaswami, K., Terk, M., and Weiss, L.E., 1994, "Shape Deposition Manufacturing," *Proceedings, Solid Freeform Fabrication Symposium*, The University of Texas at Austin, pp. 1-8.

Thomas, B.G., Samarasekera, I.V., and Brimacombe, J.K., 1987, "Mathematical Modeling of the Thermal Processing of Steel Ingots: Part II. Stress Model," *Metallurgical Transactions B*, Vol. 18B, pp. 131-147.

Touloukian, Y.S. (ed.), 1967, *Thermophysical Properties of High Temperature Solid Materials*, Macmillan, New York.

Zabaras, N., Ruan, Y., and Richmond, O., 1991, "On the Calculation of Deformations and Stresses During Axially Symmetric Solidification," *Journal of Applied Mechanics*, Vol. 58, pp. 865-871.